

Electronic Conductivity of Semiconductor Nanoparticle Monolayers at the Air|Water Interface

Ivan A. Greene,[†] Fanxin Wu,[‡] Jin Z. Zhang,[‡] and Shaowei Chen^{*,†}

Department of Chemistry and Biochemistry, Southern Illinois University, Carbondale, Illinois 62901, and Department of Chemistry and Biochemistry, University of California, Santa Cruz, California 95064

Received: December 11, 2002

The electronic conductivity of PbS and CdTe nanoparticle monolayers was examined voltammetrically by using interdigitated array (IDA) electrodes at the air|water interface. Their band gap energies were estimated from the $I-V$ responses and were very consistent with results obtained from optical measurements as well as solution electrochemistry. For CdTe nanoparticles, the $I-V$ responses were analogous to those of a molecular diode with reproducible voltammetric behavior after repeated potential cycling. Interestingly, there appeared to be indications of particle surface trap states in the voltammetric responses that correlated with spectroscopic measurements. In addition, the band gap of the nanoparticle monolayers could be manipulated by the interparticle interactions, red shifting with decreasing interparticle separation. In contrast, the electroactive nature of the PbS particles led to the decomposition of the nanoparticles and hence deposition onto the electrode surface. The resulting voltammetric responses evolved from those typical of the faradaic reactions to a rectifying feature of much larger current scales, which finally became linear (ohmic) because of shorting between neighboring IDA fingers. In these studies, it was found that photoexcitation played an important role in regulating the current responses, providing a mechanistic basis on which to manipulate the electronic/electrical properties of semiconductor nanomaterials. The conductivity of the final interfinger deposits was about 2 orders of magnitude smaller than that for pure metallic lead, indicating some surface contamination and/or less than perfect crystalline structure.

Introduction

The recent intense interest in nanoscale materials is mainly driven by their unique properties that can be easily manipulated by their physical dimensions and surface morphology as well as their chemical environment.¹ In addition, in organized ensemble structures, the distribution and ordering of the particle molecules play an important role in regulating the electronic properties of the overall assemblies.² These will be the key structural parameters in the fabrication of novel electronic nanodevices and nanocircuits. For instance, Heath and co-workers measured the nonlinear optical properties of a Langmuir monolayer of alkanethiolate-protected silver nanoparticles and observed an insulator–metal transition when the interparticle spacing was reduced by mechanical compression.³ This was interpreted by the distance dependence of electronic coupling between neighboring particle molecules. More recently, using an interdigitated array (IDA) electrode, we directly measured the electronic conductivity of alkanethiolate-protected gold nanoparticles at the air|water interface.⁴ For particles with protecting monolayers of short-chain ligands, we observed ohmic current–potential ($I-V$) responses whereas for longer chain lengths nonlinear $I-V$ curves were generally found to have rectifying character. This discrepancy in electronic properties could not be interpreted solely on the basis of interparticle distance. More likely, it was related to the combined effects of organic insulating layers on particle electronic interactions as

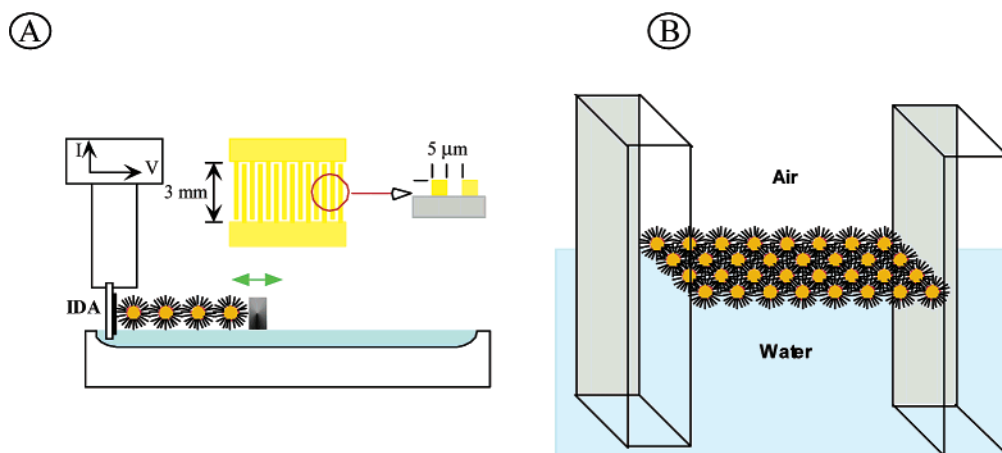
well as on a variation in electron-transfer mechanisms (e.g., tunneling, hopping, or metallic). In addition, these observations are in sharp contrast with previous studies of solid-state conductivity measurements using drop-cast (μm) thick films of nanoparticles where generally only ohmic responses were found.^{5,6} This latter observation was, at least in part, attributable to the structural inhomogeneity in the particle thick films where effective electron-transfer pathways might be facilitated by film defects.

Previous efforts have been mainly focused on transition-metal nanoparticles, whereas studies of the electronic conductivity of semiconductor nanoparticle materials are relatively scarce.^{7,8} For instance, Otten et al.^{7a} measured the current noise spectra of PbS nanoparticle thin films, which indicated a random walk (diffusion) of electrons between the particles. Alperson et al.^{7b} used a conductive scanning force microscope to investigate the electronic conductance of isolated CdSe quantum dots where the nanoparticle band gap as well as Coulomb charging were evaluated. Mallouk and co-workers⁸ fabricated a nanoscale heterojunction with semiconductor nanoparticles and observed rectifying current responses. Of these studies, one of the intriguing properties associated with semiconductor nanoparticles is their band gap energy, which has been found to be sensitive to particle dimensions because of quantum confinement effects as well as to the chemical environment of the particles. Because a variety of nanoparticle properties (optical, luminescence, electronic, etc.) are dependent upon this band gap energy, an accurate assessment is of paramount importance in understanding the molecular mechanism. Typically, this energy is characterized by optical measurements (e.g., UV–vis spectro-

* To whom all correspondence should be addressed. E-mail: schen@chem.siu.edu.

[†] Southern Illinois University.

[‡] University of California.

SCHEME 1 ^a

^a (A) Experimental setup for electronic conductivity measurements at the air|water interface (not to scale).⁴ (B) Schematic of the IDA fingers and the nanoparticle monolayers.

copy).⁹ Recently, it was found that electrochemistry was also an effective complementary tool where the nanoparticle band gap was reflected by a featureless current profile in voltammetric measurements.^{10,11} However, for many nanosized semiconductor materials, the band gap typically lies in the range of a few electron volts, sometimes rendering it difficult to evaluate this energy structure in solutions using conventional electrochemical approaches because of limited access to suitable solvents. Solid-state electrochemical approaches offer an effective alternative.

In this article, we will report on the electronic conductivity measurements of semiconductor nanoparticle monolayers at the air|water interface by using monolayer-protected PbS and CdTe nanoparticles as the illustrating examples. We will first focus on their solid-state electron-transfer chemistry and then examine the effects of interparticle separation on the band gap energies of nanoparticle ensembles. More significantly, we will demonstrate that nanoparticle trap states can be located by combining voltammetric results with spectroscopic data.

Experimental Section

The synthesis of *n*-hexanethiolate-protected PbS nanoparticles has been described in detail in a previous report.¹¹ CdTe nanoparticles used in the present study were stabilized first by a monolayer of thioglycolic acid in aqueous solutions and rendered hydrophobic by binding to a second layer of dimethyldioctadecylammonium. The synthesis of thiol-capped CdTe in aqueous solutions was also detailed in earlier articles.¹² The average core sizes of these two nanoparticles were ca. 4 and 2 nm, respectively, with a very narrow dispersity (standard deviation of about 15% of the average particle size), as determined by transmission electron microscopy.

UV-vis absorption spectra were acquired with a Unicam ATI UV4 spectrometer, and fluorescence studies were carried out with a PTI fluorescence spectrometer. The particle solutions were prepared in CHCl_3 at a concentration of approximately $2.75 \mu\text{M}$.

In both cases, a monolayer of the nanoparticle molecules was formed at the air|water interface using the Langmuir technique (NIMA 611D). For PbS nanoparticles, typically $250 \mu\text{L}$ of the particle solutions ($2.75 \mu\text{M}$ CH_2Cl_2) was spread dropwise onto the water surface. At least 20 min was allowed for solvent evaporation as well as between compression cycles. An interdigitated array (IDA, from ABTECH Scientific) electrode was aligned vertically at the air|water interface where a monolayer

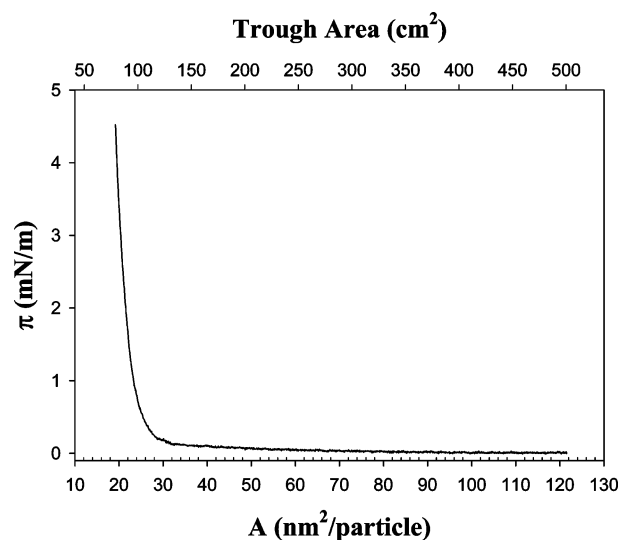


Figure 1. Langmuir isotherm of PbS nanoparticles. *n*-Hexanethiolate-protected PbS nanoparticles were dissolved in CH_2Cl_2 at a concentration of $2.75 \mu\text{M}$. This solution ($250 \mu\text{L}$) was spread dropwise onto the water surface. Compression speed $20 \text{ cm}^2/\text{min}$.

of nanoparticles was trapped between IDA fingers. (Details of the experimental setup are shown in Scheme 1, as described previously⁴). The IDA electrode consists of 25 pairs of gold fingers with dimensions of $3 \text{ mm} \times 5 \mu\text{m} \times 5 \mu\text{m}$ ($L \times W \times H$). The corresponding current-potential ($I-V$) profiles were collected directly at the air|water interface by applying a voltage bias to the contacts of the finger pairs using an EG&G PARC potentiostat (model 283) and EG&G commercial software (PowerCV).

Results and Discussion

Figure 1 shows the Langmuir isotherm of PbS nanoparticles on the water surface. One can see that at trough areas greater than $26 \text{ nm}^2/\text{particle}$ the surface pressure is essentially zero, equivalently indicating a 2D gaseous state of the particle molecules whereas at a smaller surface area the pressure starts to rise rather rapidly, suggesting that the particles are in close contact and ligand intercalation starts to occur. At this takeoff area, on the basis of a hexagonal arrangement within the particle monolayers, the average interparticle center-to-center distance can be estimated to be about 5.61 nm , which is only slightly larger than the physical diameter of the PbS particles (core +

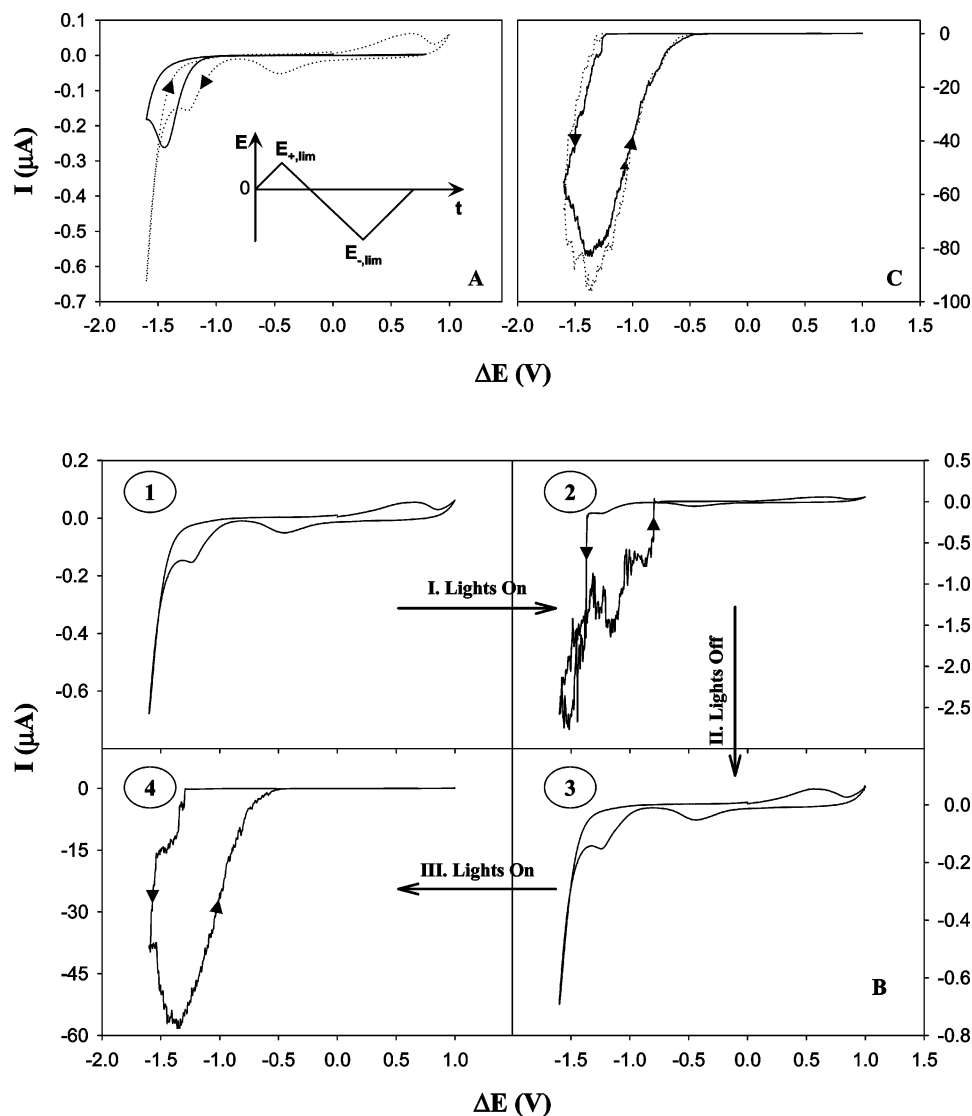
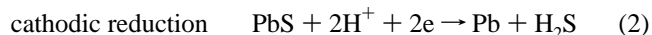
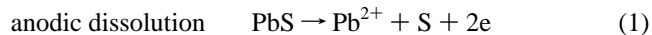


Figure 2. (A) Current–voltage profiles of PbS nanoparticle monolayers at $\pi = 3$ mN/m in the dark. Potential scan rate 10 mV/s. (B) Effects of photoexcitation (red light) on the electronic conductivity of PbS nanoparticles. Potential scan rate 20 mV/s. (C) Current–potential profiles in the dark after photoexcitation as described in B. Potential scan rate 20 mV/s. The inset in A depicts the potential program, where $E_{+,lim}$ and $E_{-,lim}$ denote the positive and negative limits of the potential range, respectively.

two fully extended chains of hexanethiolates with 0.78 nm each as calculated by Hyperchem). The overall behaviors are quite similar to those of alkanethiolate-protected gold nanoparticles.⁴

The corresponding current–voltage profiles are shown in Figure 2A with varied potential windows (with surface pressure-controlled at 3 mN/m, i.e., the interparticle edge-to-edge spacing (L) is about 0.97 nm). The potential scanning program is shown in the Figure 2A inset. One can see that within the potential range of -1.0 and $+0.8$ V the current response ($-$), on the order of a few nanoamps, is essentially featureless. However, when the negative potential is expanded to -1.6 V ($-$), a cathodic peak appears at around -1.45 V with no apparent return wave. In addition, when the positive potential is simultaneously expanded to $+1.0$ V ($. . .$), an anodic peak starts to show up at ca. $+0.7$ V, and on the return (cathodic) scan, a new peak appears at -0.5 V in addition to the original cathodic peak observed in the previous potential window (which now shifts to -1.25 V). These behaviors are very similar to those observed in electrochemical studies of PbS nanoparticles in solutions.¹¹ These voltammetric features are ascribed to the charge-transfer reactions involved in PbS decomposition. It has been rather well known that PbS undergoes decomposition

processes at very negative and positive potentials by the following reaction mechanisms:¹¹



Thus, one can see that the voltammetric peak at -1.25 V is most likely related to the cathodic reduction of PbS nanoparticles (2) leading to the deposition of metallic Pb onto the electrode surface whereas the anodic peak at $+0.7$ V is attributable to the anodic dissolution of PbS nanoparticles (1) and the voltammetric peak (-0.5 V) on the subsequent cathodic scan might be ascribed to the formation of Pb from Pb^{2+} generated in reaction 1. In contrast, when the electronic conductivity was measured in vacuo on a solid substrate, PbS nanoparticles were found to be stable even at a much higher voltage bias (e.g., up to 10 V).^{7a} It should be noted that the above interpretation is oversimplified because the alkanethiolate ligands have not been taken into account. Because of the hydrophobic nature of these alkanethiolate molecules, it is most likely that they stay at the air/water interface, and some might be even adsorbed to the IDA gold finger surfaces.

From these I - V measurements, one can also estimate the PbS nanoparticle band gap energy. For instance, Figure 2A depicts a flat current profile within the central potential region from -1.0 to $+0.8$ V, indicating a band gap of about 1.8 eV. This is very consistent with that evaluated voltammetrically in PbS nanoparticle solutions.¹¹ In addition, the roughly symmetric current onset about the zero voltage bias suggests that the Fermi level is located in the middle of the gap (at zero voltage bias).⁷

More interestingly, photoexcitation appears to exert rather substantial impacts on the electronic conductivity of the PbS nanoparticle monolayers. Figure 2B shows the variation of the particle voltammetric currents (within the potential range of -1.6 to $+1.0$ V) with and without exposure to a red light source (650 nm, <5 mW).¹³ When the particle monolayer was exposed to the light source, the corresponding current maximum increases about 4-fold (panel 1 to 2). Additionally, the current profile exhibits rectifying character (molecular diode). One can see that on the cathodic scan the onset potential is about -1.35 V whereas on the return (anodic) scan it is located at -0.8 V. This hysteresis is associated with the reductive decomposition of PbS nanoparticles at the electrode interface, which behaves rather irreversibly. Upon switching off the light source (panel 3), the I - V response returns to that before photoexcitation (panel 1), and subsequently turning on the light (panel 3 to 4) again results in a rectifying I - V curve with a hysteresis akin to that of panel 2. It should be noted that at this point the current scale is much larger (in panel 4, the current maximum is close to $60 \mu\text{A}$, about 100-fold larger than that in panel 1), suggesting an avalanching decomposition process of the PbS nanoparticles. Turning off the light source at this point did not lead to the restoration of the I - V response to the original profile. Figure 2C shows the I - V curves from subsequent scans measured in the dark. One can see that the cathodic peak currents increase gradually with repetitive cycling of the potentials, and the overall current profiles maintain rectifying behavior. (In a comparative study where the I - V curves were acquired in the dark (not shown), the current increase was much less drastic, indicating photocatalytic effects of PbS degradation.)

Further cycling of the potential bias within the range of -1.6 to $+1.0$ V leads to a drastic change in the I - V profiles (Figure 3). First, one can see that eventually the current increases by about 5 orders of magnitude and the I - V profiles start a transition to become linear (ohmic), as shown from the top to the bottom panel. This sudden transition is due to the decomposition of PbS nanoparticles and consequently the deposition of Pb onto the electrode surfaces, where repetitive cycling of the potential bias leads to the propagation of the surface deposit and the eventual shorting of the neighboring fingers. It should be noted that this final transition might be manifested explicitly in Figure 3. Here the potential scan is started first from zero to the positive end ($+1.0$ V), and the corresponding current is very small (on the present current scale). A similar current feature was observed when the potential was reversed and scanned negatively up to -1.0 V. At -1.05 V, however, there is a rather large current step ($\sim 1300 \mu\text{A}$), followed by a current plateau up to -1.2 V where another even larger current step ($\sim 1800 \mu\text{A}$) occurs. After this, the current profile becomes linear, especially in the final anodic scan. A similar current step can also be observed in the following potential cycling (center panel) with the step height ($\sim 1500 \mu\text{A}$) close to those observed in the top panel. It is very likely that these current steps represent the final fillings of the gaps between neighboring finger pairs. Once the gaps are filled, the I - V profiles become linear within the entire potential range (bottom panel), indicating ohmic charac-

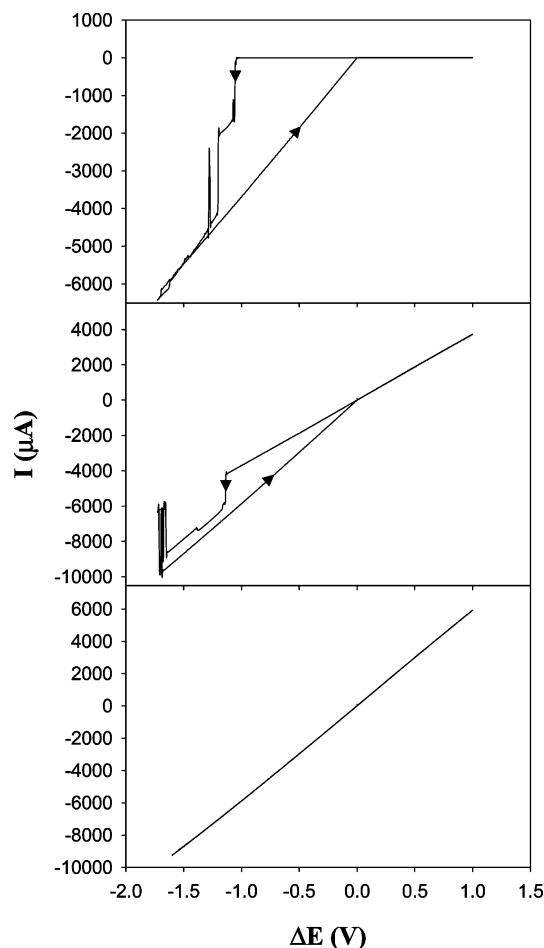


Figure 3. I - V curves of PbS nanoparticles in the dark after continuous cycling of potentials within the range of -1.6 to $+1.2$ V. Potential scan rate 20 mV/s. The potential program is the same as that shown in the Figure 2A inset.

teristics of the cathodic deposits. It should be noted that further cycling of the potential bias does not lead to an apparent increase in the voltammetric currents. This can be interpreted on the basis of the mass transport of nanoparticle molecules at the air|water interface where the interfinger deposits are most probably limited to those originally trapped between the neighboring fingers. By assuming that the thickness of the deposit is equal to the diameter of a single PbS nanoparticle, the conductivity evaluated from the slopes of these linear I - V profiles is about $3.01 \times 10^2 \text{ S cm}^{-1}$, which is about 2 orders of magnitude smaller than that of pure metallic Pb at room temperature, $4.74 \times 10^4 \text{ S cm}^{-1}$.¹⁴ This can be attributed to the less perfect structure of the surface deposit as well as possible contamination by sulfur and thiolates at the interface.

For CdTe nanoparticles, the I - V responses are quite different. Unlike PbS nanoparticles, which are prone to electrodeposition as described above, CdTe nanoparticles are much more stable under electrochemical perturbation. Figure 4 shows the I - V responses of a CdTe nanoparticle monolayer at varied surface pressures, 15 and 30 mN/m. (See Supporting Information for the Langmuir isotherm.) At these two surface pressures, the interparticle spacings (L) are about 4.23 and 3.59 nm, respectively. One should note that the thickness of the organic protecting layer of the CdTe particles (consisting of a bilayer of thioglycolate and dimethyl-dioctadecylammonium) is about 2.66 nm, thus the degree of ligand intercalation is comparable to that of the aforementioned PbS experiments. One can see that except for the broad (anodic) peaks at around $+0.95$ and

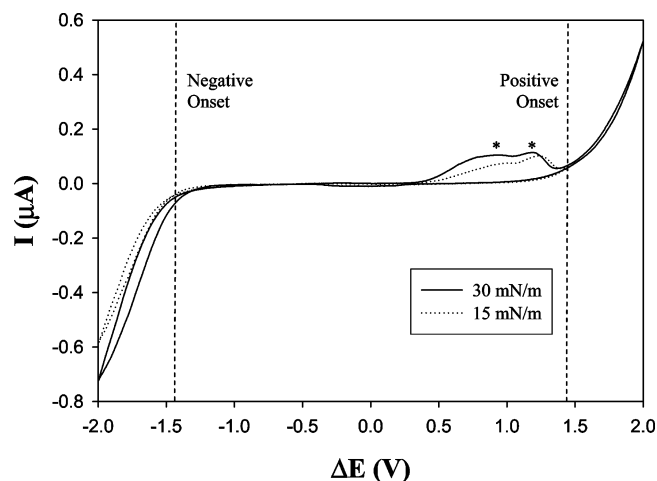


Figure 4. Current–potential curves of CdTe nanoparticle monolayers at varied surface pressures: 15 and 30 mN/m. Potential scan rate 10 mV/s. The potential program is the same as in the Figure 2A inset. Asterisks indicate the positions of the two prominent voltammetric peaks. Dashed lines denote the positions of the positive and negative onset potentials.

+1.2 V (indicated by asterisks in Figure 4), the current responses are rather analogous to those of a molecular diode: within the large central potential range (ca. -1.45 to $+1.45$ V), the current is essentially zero, whereas at more negative or positive potentials the currents start to increase rather rapidly. It has to be mentioned that the exact origin is not clear at this point regarding the voltammetric peaks at $+0.95$ and $+1.2$ V (indicated by asterisks), which appear to be electrochemically irreversible. In a previous report¹⁵ involving surface multilayers of CdTe nanoparticles, similar voltammetric responses were also observed. However, the authors did not elaborate upon the possible cause for the observations. One possible interpretation is that the voltammetric peaks arise from the electrodegradation of CdTe particles, akin to those observed with PbS particles (vide ante). However, the I – V responses are very reproducible after repeated cyclings of potential bias, suggesting that the

particles trapped between neighboring IDA fingers are quite stable. Another plausible explanation is that these voltammetric features are due to CdTe particle surface trap states, which is further supported by spectroscopic measurements, as explained below.

Figure 5 shows the UV–vis absorption and fluorescence spectra of the CdTe nanoparticles dissolved in CHCl_3 . One can see that there is a quite well-defined excitonic absorption peak at 412 nm, and the fluorescence profile exhibits a rather broad peak at 594 nm (when excited at 400 nm). For particles of similar core size, band-edge luminescence (BEL, Scheme 2) is anticipated to peak at ca. 500 nm with a much narrower peak width (i.e., behaving as a direct band gap material), as observed previously.¹² The observation of an emission peak at a much longer wavelength position (594 nm) strongly suggests that it arises mainly from surface trap states. In fact, when the fluorescence profile in Figure 5 is fitted by a Gaussian waveform, one can see quite clearly that in addition to the main peak at 594 nm there is a small but quite well-defined one at 500 nm (details in Figure S2 of Supporting Information), indicating the contributions from both modes of electronic transitions.

It should be noted that the energy difference between these two fluorescence peaks is about 0.4 eV, indicating that the trap state is located either 0.4 eV above the valence band or 0.4 eV below the conduction band. Another possibility is that the deviation is the combined shifts in energy of both the electron and hole trap states. Because the band gap can be defined by the difference between the negative and positive onset potentials (vide infra), any of these shifts should be manifested in voltammetric measurements within these two onset potentials. One might notice that the voltammetric feature (observed between $+0.5$ and $+1.5$ V, indicated by two asterisks in Figure 4) was centered at ~ 1.0 V (i.e., a deviation of about 0.4 V from the positive onset potential (valance band edge)); it appears reasonable to suggest that it arises from the (surface trap) energy states that are responsible for the fluorescence emission peaking at 594 nm. Thus, from these voltammetric and spectroscopic

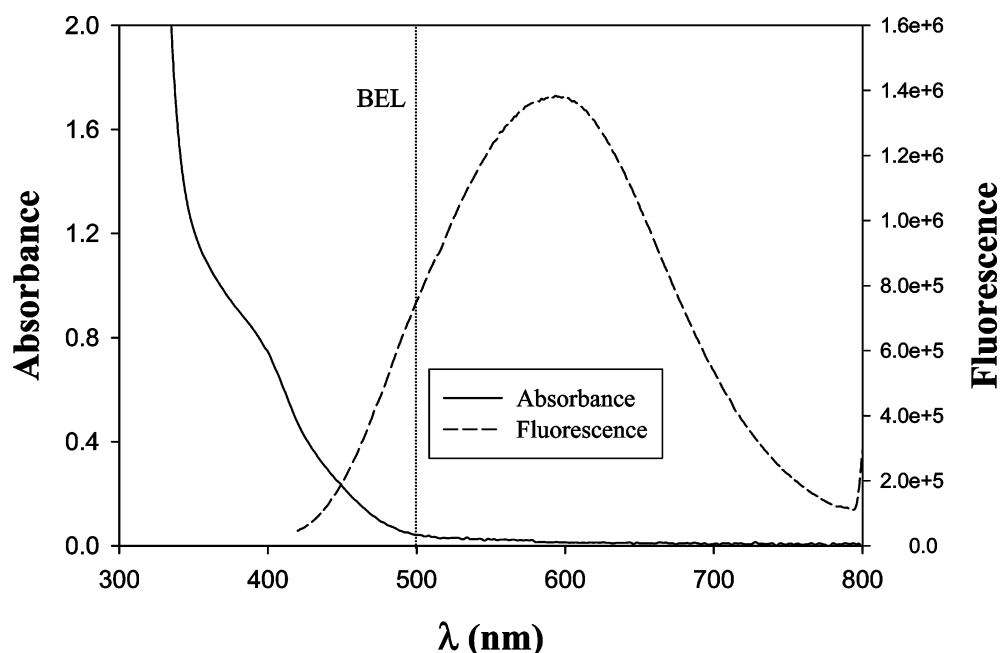
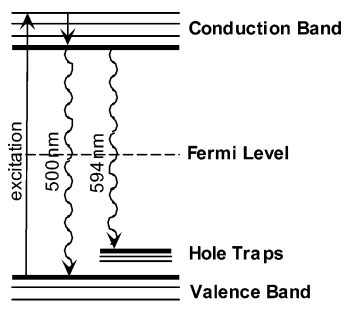


Figure 5. UV–vis absorption and fluorescence spectra of CdTe nanoparticles in CHCl_3 (0.43 mM). The fluorescence emission spectrum was collected with an excitation wavelength of 400 nm. The dotted line indicates the position of the band-edge luminescence (BEL). Details of the Gaussian fit can be found in the Supporting Information.

SCHEME 2: Schematic of the CdTe Nanoparticle Energy Structure



measurements, one can construct an energy diagram for the CdTe nanoparticles with hole trap states located near the valence band (Scheme 2). The reason for suggesting hole trap states over electron trap states is that the voltammetric peak attributed to trap states was observed near the positive onset potential (valence band edge). If this explanation is correct, then this type of electrochemical measurement of trap state energetics and positions offers some unique advantages over spectroscopic techniques, which usually cannot provide information about the exact locations of the trap states.

Furthermore, one might note that the full width at half-maximum (fwhm) of this fluorescence peak is more than 180 nm, which is significantly larger than that (38 nm) observed previously with particles of direct band gap character.^{12a} This suggests a rather broad distribution of the particle surface energy states, as observed previously.¹⁶ This can also be associated with the appearance of multiple (and broad) voltammetric peaks as observed in Figure 4. Additionally, as voltammetric currents reflect the density of states at a specific potential, one might, in principle, be able to exploit simple voltammetric measurements to evaluate the density of states of surface trap sites of semiconductor quantum dots. Further studies of this issue are underway.

From these $I-V$ measurements (Figure 4), one can also evaluate the band gap of the nanoparticle ensembles and, more significantly, manipulate the band gap by varying the interparticle spacing. At low surface pressure (15 mN/m), the band gap is about 2.93 eV, whereas at higher surface pressure (30 mN/m) the band gap is found to decrease by about 0.1 eV (at 2.83 eV) along with a slight increase in the voltammetric currents. This might be understood in terms of electronic coupling between neighboring particles, which is akin to the red shift of the surface plasmon resonance of transition-metal nanoparticle aggregates.⁴ It should be noted that interparticle electronic coupling might also account for the observation that both values are slightly smaller than that estimated from UV-vis absorption measurements of CdTe particles dissolved in solution (3.01 eV, Figure 5). A similar red shift was also observed when CdS nanoparticles were aggregated into micrometer-sized crystals as compared to that when the particles were dispersed in solution.¹⁷ Additionally, shorter interparticle spacings (higher surface pressures) lead to reduced electron-transfer tunneling barriers and hence enhanced current responses (Figure 4).⁴ It is also interesting that from the $I-V$ curves in Figure 4 interparticle interactions primarily affect the conduction band edge rather than the valence band edge. Thus, one can envision that in addition to the physical dimensions⁹ interparticle interaction (separation) is another important structural parameter in the manipulation of the optical and electronic properties of semiconductor quantum dots, and this can be achieved simply by the Langmuir technique.¹⁸

Because the positive and negative onset potentials are rather symmetric about the zero bias (even at different interparticle separations), the Fermi level of the nanoparticle ensembles is also located in the middle of the energy gap (Scheme 2), similar to that of PbS particles (vide ante).

Conclusions

In summary, by using Langmuir monolayers at the air|water interface, the electronic conductivity and band gap energy as well as surface trap states of semiconductor nanoparticles can be readily examined from the $I-V$ responses. The results are found to be very consistent with those obtained from optical measurements as well as solution electrochemistry, indicating that solid-state electrochemistry based on the Langmuir technique is an effective alternative in evaluating the energy structure of semiconductor nanoparticles. Furthermore, it is found that in addition to the chemical structure of the nanoparticle molecules, the interparticle spacing and photoexcitation are two additional important parameters by which the conductivity properties of semiconductor nanomaterials can be manipulated. Overall, studies along this line might provide some fundamental insight into the mechanism of electrochromic/electroluminescence processes involving semiconductor nanoparticles.¹⁹

Acknowledgment. We are grateful to Mr. S. Liu for his assistance in data collection in the early stage of the experiments. This work was supported, in part, by the National Science Foundation (CAREER Award CHE-0092760, S.C.), the ACS Petroleum Research Fund (S.C. and J.Z.Z.), the Materials Research Institute of Lawrence Livermore National Labs (J.Z.Z.), and the SIU Materials Technology Center (S.C.). S.C. is a Cottrell Scholar of the Research Corporation.

Supporting Information Available: Langmuir isotherm of CdTe nanoparticle monolayers and Gaussian fitting of the CdTe fluorescence profile. This information is available free of charge via the Internet at <http://pubs.acs.org>.

References and Notes

- (1) (a) Schmid, G. *Clusters and Colloids: From Theory to Applications*; VCH: New York, 1994. (b) *Clusters of Atoms and Molecules*; Haberland, H., Ed.; Springer-Verlag: New York, 1994. (c) Turton, R. *The Quantum Dot: A Journey into the Future of Microelectronics*; Oxford University Press: New York, 1995.
- (2) Remacle, F.; Levine, R. D. *Chem. Phys. Chem.* **2001**, *2*, 20 and references therein.
- (3) Markovich, G.; Collier, C. P.; Henrichs, S. E.; Remacle, F.; Levine, R. D.; Heath, J. R. *Acc. Chem. Res.* **1999**, *32*, 415 and references therein.
- (4) Chen, S. *Anal. Chim. Acta*, in press.
- (5) (a) Wuelfing, W. P.; Murray, R. W. *J. Phys. Chem. B* **2002**, *106*, 3139. (b) Wuelfing, W. P.; Green, S. J.; Pietron, J. J.; Cliffel, D. E.; Murray, R. W. *J. Am. Chem. Soc.* **2000**, *122*, 11465.
- (6) (a) Evans, S. D.; Johnson, S. R.; Cheng, Y. L.; Shen, T. *J. Mater. Chem.* **2000**, *10*, 183. (b) Doty, R. C.; Yu, H.; Shih, C. K.; Korgel, B. A. *J. Phys. Chem. B* **2001**, *105*, 8291. (c) Snow, A. W.; Wohltjen, H. *Chem. Mater.* **1998**, *10*, 947. (d) Clarke, L.; Wybourn, M. N.; Brown, L. O.; Hutchison, J. E.; Yan, M.; Cai, S. X.; Keana, J. F. W. *Semicond. Sci. Technol.* **1998**, *13*, A111.
- (7) (a) Otten, F.; Kish, L. B.; Vandamme, L. K. J.; Vajtai, R.; Kruis, F. E.; Fissan, H. *Appl. Phys. Lett.* **2000**, *77*, 3421. (b) Alperson, B.; Cohen, S.; Rubinstein, I.; Hodes, G. *Phys. Rev. B* **1995**, *52*, R17017.
- (8) (a) Kovtyukhova, N. I.; Martin, B. R.; Mbindyo, J. K. N.; Smith, P. A.; Razavi, B.; Mayer, T. S.; Mallouk, T. E. *J. Phys. Chem. B* **2001**, *105*, 8762. (b) Cassagneau, T.; Mallouk, T. E.; Fendler, J. H. *J. Am. Chem. Soc.* **1998**, *120*, 7848.
- (9) (a) Bawendi, M. G.; Steigerwald, M. L.; Brus, L. E. *Annu. Rev. Phys. Chem.* **1990**, *41*, 477. (b) Alivisatos, A. P. *J. Phys. Chem.* **1996**, *100*, 13226.
- (10) Haram, S. K.; Quinn, B. M.; Bard, A. J. *J. Am. Chem. Soc.* **2001**, *123*, 8860.
- (11) Chen, S.; Truax, L. A.; Sommers, J. M. *Chem. Mater.* **2000**, *12*, 3864.

(12) (a) Wu, F.; Lewis, J. W.; Klinger, D. S.; Zhang, J. Z. *J. Chem. Phys.* **2003**, *118*, 12. (b) Dirk, G.; Kurth, P. L.; Lesser, C. *Chem. Commun.* **2000**, 949.

(13) These PbS nanoparticles can be photoexcited for luminescence emission by a wavelength shorter than 700 nm (details in ref 11).

(14) *Handbook of Chemistry and Physics*; Lide, D. R., Ed.; CRC Press: Boca Raton, FL, 1996.

(15) Gao, M.; Sun, J.; Dulkeith, E.; Gaponik, N.; Lemmer, U.; Feldmann, J. *Langmuir* **2002**, *18*, 4098.

(16) (a) Zhang, J. *J. Phys. Chem. B* **2000**, *104*, 7239. (b) Gao, M.; Kirstein, S.; Mohwald, H.; Rogach, A. L.; Kornowski, A.; Eychmuller, A.; Weller, H. *J. Phys. Chem. B* **1998**, *102*, 8360. (c) Becker, W. G.; Bard, A. *J. Phys. Chem.* **1983**, *87*, 4888.

(17) Döllefeld, H.; Weller, H.; Eychmuller, A. *Nano Lett.* **2001**, *1*, 267.

(18) Photoexcitation is also found to affect the I - V properties of CdTe nanoparticles. However, the effects appear to be contingent upon the range of applied potential bias. When the bias voltage is smaller than the band gap, excitation by ambient light leads to a small but visible increase in the voltammetric currents. However, when the applied bias voltage is larger than the band gap, virtually no effect is observed from photoexcitation by ambient light, indicating that within this experimental context electron transfer is mainly driven by electrode potentials.

(19) (a) Shim, M.; Guyot-Sionnest, P. *Nature* **2000**, *407*, 981. (b) Woo, W.-K.; Shimizu, K. T.; Jarosz, M. V.; Neuhauser, R. G.; Leatherdale, C. A.; Rubner, M. A.; Bawendi, M. G. *Adv. Mater.* **2002**, *14*, 1068.